DEPARTMENT OF AEROSPACE ENGINEERING
COLLEGE OF ENGINEERING & TECHNOLOGY
OLD DOMINION UNIVERSITY
NORFOLK, VA 23529

EXPERIMENTAL AND NUMERICAL ANALYSIS OF STRUCTURAL ACOUSTICCONTROL INTERIOR NOISE REDUCTION

By

Dr. Chuh Mei, Principal Investigator
Jeffrey S. Bevan, Graduate Research Assistant
Department of Engineering & Technology

FINAL REPORT
For the period ending January 9, 1999

Prepared for
NASA Langley Research Center
Attn.: Travis L. Turner
Technical Officer
Mail Stop 463
Hampton, VA 23681

June 1999

FORWARD

The research results contained in this technical report were performed under the NASA grant NAG-1-1684 entitled "Experimental and Numerical Structural Acoustic Control for Interior Noise Reduction". The report is based essentially on partial progress of the Ph. D. dissertation prepared by Jeffrey S. Bevan under direct guidance of Dr. Chuh Mei. The document presents a finite element formulation and control of sound radiated from cylindrical panels embedded with piezoceramic actuators. The extended MIN6 shallow shell element is fully electrical-structural coupled. A piezoelectric modal actuator participation (PMAP) is defined which indicates the actuator performance to each of the offending modes. Genetic algorithm is also employed to validate the sensor and actuator locations determined by the PMAP criteria. The work was conducted at the Department of Aerospace Engineering, Old Dominion University. Mr. Travis L. Turner, Structural Acoustics Branch, NASA Langley Research Center is the technical monitor. The research is continued under the new grant NAG-1-2141.

TABLE OF CONTENTS

1. Shallow Shell Finite Element Formulation

The three-node shallow shell element presented is an extension of the MIN6 developed by Tessler[1]. A brief description of the element attributes includes 3-node shallow curved shell triangle with fifteen nodal degrees-of-freedom (dof). The element employs C^o anisoparametric interpolation to account for both membrane and transverse nodal displacement. The membrane and transverse displacement each utilize unique interpolation polynomials, which offer distinctly different polynomial degrees as introduced by Tessler[2]. The transverse displacement employs a complete quadratic polynomial, while the bending rotations utilizes a linear interpolation scheme. The MIN6 formulation consists of a Marguerre shallow shell membrane strain consistent with the Reissner-Mindlin theory which includes transverse shear effects. Static condensation eliminates the extra nodes required to facilitate the complete quadratic polynomials while maintaining the minimum specified number of nodal dof. By formulating a co-rotational highly nonlinear solution, Barut[3] et al exhibits the versatility of the MIN6 shallow shell element. This research further expands the MIN6 capability by including anisotropic piezoceramic materials in conjunction with unsymetric laminated composite resulting in a fully electrical-structural coupled shallow shell finite element formulation.

2. Element Displacement Functions

Displacement field components u_x, u_y, and u_w, consistent with Mindlin theory, are described as

$$u_x = u(x,y,t) + \bar{z}\theta_y(x,y,t)$$
$$u_y = v(x,y,t) + \bar{z}\theta_x(x,y,t) \qquad (2.1)$$
$$u_w = w(x,y,t)$$

1

where u, v, w represent the mid-surface membrane and transverse displacements; bending rotations of the normal about the x and y axes are given by θ_x and θ_y respectively. The element coordinate system is defined as positive x along the side between nodes 1-2 as shown in Figure 1. The arbitrary shallow shell shape is described by $h_o(x,y)$ and related to the z-axis as
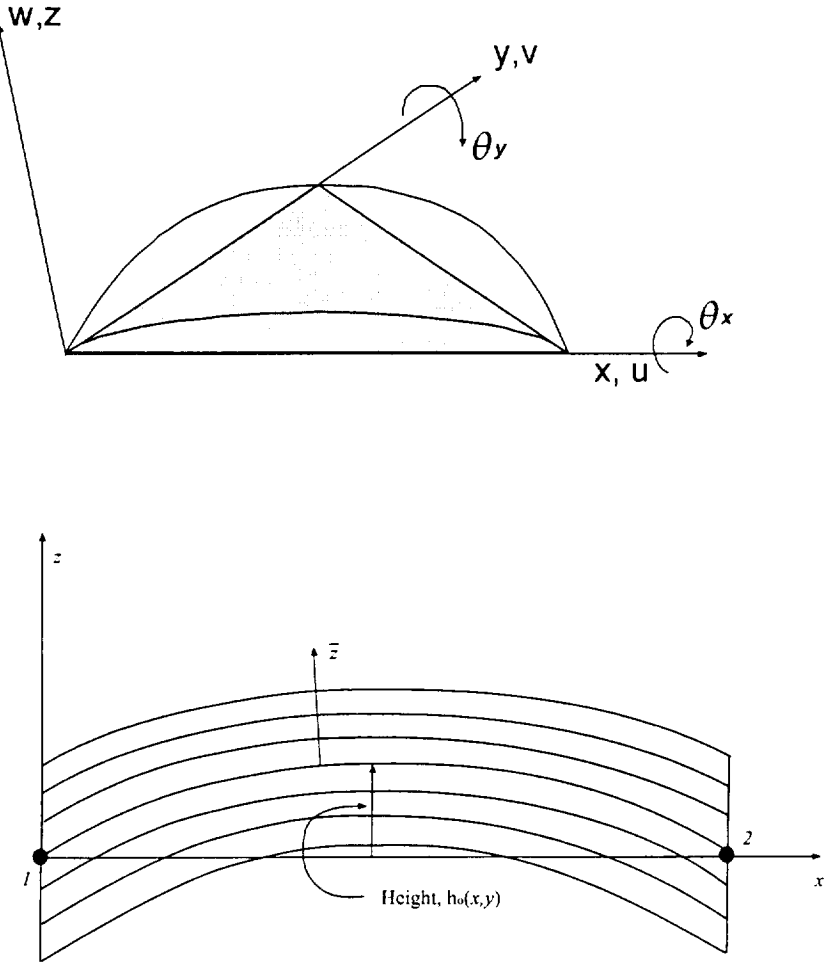
$$\overline{z} = z - h_o(x, y)$$

Figure 1 MIN6 Geometric description

Thus, the nodal displacement vectors can be written as

$$\{w\}^T = \left\{ \lfloor w_b \rfloor \quad \lfloor \theta \rfloor \quad \lfloor w_m \rfloor \quad \lfloor w_\phi \rfloor \right\} \tag{2.2}$$

$$\{w_b\}^T = \lfloor w_1 \quad w_2 \quad w_3 \rfloor \tag{2.3}$$

$$\{\theta\}^T = \lfloor \theta_{x1} \quad \theta_{x2} \quad \theta_{x3} \quad \theta_{y1} \quad \theta_{y2} \quad \theta_{y3} \rfloor \tag{2.4}$$

$$\{w_m\}^T = \lfloor u_1 \quad u_2 \quad u_3 \quad v_1 \quad v_2 \quad v_3 \rfloor \tag{2.5}$$

where each electrical dof is the coupled, total electric potential of each piezoceramic layer. For example, consider np layers of piezoceramic material the electric potential dof is given by

$$\{w_\phi\}^T = \lfloor V_1 \quad \cdots \quad V_{np} \rfloor \tag{2.6}$$

Considering the inherent electrical-mechanical coupling of piezoceramics, the electrical potential dof includes both self-generated, or sensor voltage, and externally applied, or actuation voltage. The coupled piezoelectric constitutive relation is described in Sect. 4.

The displacement field throughout the element is determined by interpolating the nodal displacement as

$$\begin{aligned} w(x,y,t) &= \lfloor H_w \rfloor \{w_b\} + \lfloor H_{w\theta} \rfloor \{\theta\} \\ &= \lfloor \xi_1 \quad \xi_2 \quad \xi_3 \rfloor \{w_b\} + \lfloor L_1 \quad L_2 \quad L_3 \quad M_1 \quad M_2 \quad M_3 \rfloor \{\theta\} \end{aligned} \tag{2.7}$$

$$\theta_x(x,y,t) = \lfloor H_{\theta x} \rfloor \{\theta\} = \lfloor \xi_1 \quad \xi_2 \quad \xi_3 \quad 0 \quad 0 \quad 0 \rfloor \{\theta\} \tag{2.8}$$

$$\theta_y(x,y,t) = \lfloor H_{\theta y} \rfloor \{\theta\} = \lfloor 0 \quad 0 \quad 0 \quad \xi_1 \quad \xi_2 \quad \xi_3 0 \rfloor \{\theta\} \tag{2.9}$$

$$u(x,y,t) = \lfloor H_u \rfloor \{w_m\} = \lfloor \xi_1 \quad \xi_2 \quad \xi_3 \quad 0 \quad 0 \quad 0 \rfloor \tag{2.10}$$

$$v(x,y,t) = \lfloor H_v \rfloor \{w_m\} = \lfloor 0 \quad 0 \quad 0 \quad \xi_1 \quad \xi_2 \quad \xi_3 \rfloor \tag{2.11}$$

Natural coordinates commonly used to describe triangles refer simply to area ratios. These area or natural coordinates ξ_1, ξ_2, ξ_3 are related to the geometric coordinates by utilizing the following transformation relations

$$\begin{Bmatrix} 1 \\ x \\ y \end{Bmatrix} = \begin{bmatrix} 1 & 1 & 1 \\ x_1 & x_2 & x_2 \\ y_1 & y_2 & y_3 \end{bmatrix} \begin{Bmatrix} \xi_1 \\ \xi_2 \\ \xi_3 \end{Bmatrix}$$

(2.12)

$$\begin{Bmatrix} \xi_1 \\ \xi_2 \\ \xi_3 \end{Bmatrix} = \frac{1}{2A} \begin{bmatrix} x_2 y_3 - x_3 y_2 & y_2 - y_3 & x_3 - x_2 \\ x_3 y_1 - x_1 y_3 & y_3 - y_1 & x_1 - x_3 \\ x_1 y_2 - x_2 y_1 & y_1 - y_2 & x_2 - x_1 \end{bmatrix} \begin{Bmatrix} 1 \\ x \\ y \end{Bmatrix}$$

where (x_i, y_i) designate the ith nodal coordinate, and the triangular area A is given by

$A = \frac{1}{2}\left((x_2 - x_1)(y_3 - y_1) - (x_3 - x_1)(y_2 - y_1)\right)$. The interpolation functions are defined as follows

$$L_1 = \frac{1}{8}(b_3 N_4 - b_2 N_6) \quad L_2 = \frac{1}{8}(b_1 N_5 - b_3 N_4)$$

$$L_3 = \frac{1}{8}(b_3 2N_6 - b_1 N_5) \quad M_1 = \frac{1}{8}(a_2 N_6 - a_3 N_4)$$

$$M_2 = \frac{1}{8}(a_3 N_4 - a_1 N_5) \quad M_3 = \frac{1}{8}(a_1 N_5 - a_2 N_6)$$

$$N_4 = 4\xi_1\xi_2 \quad N_5 = 4\xi_2\xi_3 \quad N_6 = 4\xi_3\xi_1$$

$$a_1 = x_{32} \quad a_2 = x_{13} \quad a_3 = x_{21}$$

$$b_1 = y_{32} \quad b_2 = y_{13} \quad b_3 = y_{21}$$

$$x_{ij} = x_i - x_j \quad y_{ij} = y_i - y_j$$

(2.13)

Integration of polynomials expressed in area coordinates can be accomplished with the following formula

$$\int_A \xi_k \xi_l \xi_m \, dA = 2A \frac{k!l!m!}{(2+k+l+m)!}$$

(2.14)

Geometric matrices describing the strain interpolation functions are given by the following definitions.

$$[C_m] = \begin{bmatrix} \lfloor H_u \rfloor_{,x} \\ \lfloor H_v \rfloor_{,y} \\ \lfloor H_v \rfloor_{,x} + \lfloor H_u \rfloor_{,y} \end{bmatrix} = \frac{1}{2A} \begin{bmatrix} y_{23} & y_{31} & y_{12} & 0 & 0 & 0 \\ 0 & 0 & 0 & x_{32} & x_{13} & x_{21} \\ x_{32} & x_{13} & x_{21} & y_{23} & y_{31} & y_{12} \end{bmatrix} \tag{2.15}$$

$$[C_b] = \begin{bmatrix} \lfloor H_{\theta y} \rfloor_{,x} \\ \lfloor H_{\theta x} \rfloor_{,y} \\ \lfloor H_{\theta x} \rfloor_{,x} + \lfloor H_{\theta y} \rfloor_{,y} \end{bmatrix} = \frac{1}{2A} \begin{bmatrix} 0 & 0 & 0 & y_{23} & y_{31} & y_{12} \\ x_{32} & x_{13} & x_{21} & 0 & 0 & 0 \\ y_{23} & y_{31} & y_{12} & x_{32} & x_{13} & x_{21} \end{bmatrix} \tag{2.16}$$

$$[C_{\gamma b}] = \begin{bmatrix} \lfloor H_w \rfloor_{,y} \\ \lfloor H_w \rfloor_{,x} \end{bmatrix} = \frac{1}{2A} \begin{bmatrix} x_{32} & x_{13} & x_{21} \\ y_{23} & y_{31} & y_{12} \end{bmatrix} \tag{2.17}$$

$$[C_{\gamma \theta}] = \begin{bmatrix} \lfloor H_{w\theta} \rfloor_{,y} + \lfloor H_{\theta x} \rfloor \\ \lfloor H_{w\theta} \rfloor_{,x} + \lfloor H_{\theta y} \rfloor \end{bmatrix} \tag{2.18}$$

3. Strain-Displacement Relations

Tessler[1] first developed the shallow shell element utilized by combining both Reissner-Mindlin and Marguerre theories. The Marguerre theory enforces the Kirchhoff assumption thereby neglecting shear deformation in contrast to Reissner-Mindlin theory. Substituting the normal bending rotations for the overall slope in the Reissner-Mindlin theory yields the following Marguerre inplane strain compatible to Reissner-Mindlin

$$\{\varepsilon^o\} = \begin{Bmatrix} u_{,x} \\ v_{,y} \\ u_{,y} + v_{,x} \end{Bmatrix} - \begin{Bmatrix} h_{o,x} \theta_y \\ h_{o,y} \theta_x \\ h_{o,y} \theta_y + h_{o,x} \theta_x \end{Bmatrix} \tag{3.1}$$

The following curvature and shear strain completes the strain relations

$$\{\kappa\} = \begin{Bmatrix} \theta_{y,x} \\ \theta_{x,y} \\ \theta_{y,y} + \theta_{x,x} \end{Bmatrix} \tag{3.2}$$

5

$$\{\gamma\} = \begin{Bmatrix} \gamma_{yz} \\ \gamma_{xz} \end{Bmatrix} = \begin{Bmatrix} w_{,y} \\ w_{,x} \end{Bmatrix} + \begin{Bmatrix} \theta_x \\ \theta_y \end{Bmatrix} \tag{3.3}$$

4. Constitutive Relations

The kth layer of the laminate specifies either structural or piezoceramic properties and is characterized by the following coupled constitutive relations

$$\{\sigma\}_k = [\overline{Q}]_k (\{\varepsilon\} - E_{3k}\{d\}_k) \tag{4.1}$$

$$\{\tau\} = [\overline{Q}_s]_k \{\gamma\} \tag{4.2}$$

$$D_{3k} = \{d\}_k^T [\overline{Q}]_k (\{\varepsilon^o\} - E_{3k}\{d\}_k) + \epsilon_{33k}^\sigma E_{3k} \tag{4.3}$$

$$\{E_3\} = -[B_\phi]\{w_\phi\} = - \begin{bmatrix} \dfrac{1}{h_1} & \cdots & 0 \\ \vdots & \ddots & \vdots \\ 0 & \cdots & \dfrac{1}{h_{np}} \end{bmatrix} \lfloor V_1 \quad \cdots \quad V_{np} \rfloor \tag{4.4}$$

Eq. (4.3) defines D_{3k} the kth layer electric displacement density resulting from two components, namely strain and the total electric field E_{3k}, which are coupled through the piezoelectric d coefficients. The piezoceramic layer is polarized in the 3-direction and anisotropic in the 1-2 and 1-3 material directions. Furthermore, each piezoceramic layer may have an arbitrary orientation angle. The lamina reduced stiffness components are determined from the principal material properties as

$$Q_{11} = \frac{E_1}{1 - v_{12}v_{21}} \qquad Q_{12} = \frac{v_{12}E_2}{1 - v_{12}v_{21}} \qquad Q_{22} = \frac{E_2}{1 - v_{12}v_{21}}$$

$$Q_{66} = G_{12} \qquad Q_{44} = G_{23} \qquad Q_{55} = G_{12} \tag{4.5}$$

The ability to accurately model piezoceramic anisotropy supports current research trends in advanced transducer development. If anisotropic piezoceramic material is used

the following transformation relates the principal coordinate charge coefficients to the global coordinates

$$
\begin{Bmatrix} d_x \\ d_y \\ d_{xy} \end{Bmatrix} = \begin{bmatrix} \cos^2\alpha & \sin^2\alpha & -\cos\alpha\sin\alpha \\ \sin^2\alpha & \cos^2\alpha & \cos\alpha\sin\alpha \\ 2\cos\alpha\sin\alpha & -2\cos\alpha\sin\alpha & \cos^2\alpha - \sin^2\alpha \end{bmatrix} \begin{Bmatrix} d_{31} \\ d_{32} \\ 0 \end{Bmatrix}
\tag{4.6}
$$

5. Force and Moment Resultant

Analysis of laminated composite plates maintains distinct lamina stress, therefore utilizing stress resultants is imperative. The stress resultants, or force and moment per unit length are defined as

$$
\left(\{N\}, \{M\} \right) = \int_{-h/2}^{h/2} \{\sigma\}_k (1, \bar{z}) d\bar{z}
\tag{5.1}
$$

$$
\{R\} = \int_{-h/2}^{h/2} \begin{Bmatrix} \tau_{yz} \\ \tau_{xz} \end{Bmatrix}_k d\bar{z}
\tag{5.2}
$$

Utilizing Eq.(5.1) it is useful to define the stress resultants as follows

$$
\begin{Bmatrix} N \\ M \end{Bmatrix} = \begin{bmatrix} [A] & [B] \\ [B] & [D] \end{bmatrix} \begin{Bmatrix} \varepsilon^o \\ \kappa \end{Bmatrix} - \begin{Bmatrix} N_\phi \\ M_\phi \end{Bmatrix}
\tag{5.3}
$$

where the extension, extension-bending, and bending stiffness matrices are defined as

$$
[A] = \sum_{k=1}^{n} [\bar{Q}]_k (\bar{z}_{k+1} - \bar{z}_k)
\tag{5.4}
$$

$$
[B] = \frac{1}{2} \sum_{k=1}^{n} [\bar{Q}]_k (\bar{z}_{k+1}^2 - \bar{z}_k^2)
\tag{5.5}
$$

$$
[D] = \frac{1}{3} \sum_{k=1}^{n} [\bar{Q}]_k (\bar{z}_{k+1}^3 - \bar{z}_k^3)
\tag{5.6}
$$

$$
[A_s] = \sum_{k=1}^{n} [\bar{Q}_s] (\bar{z}_{k+1} - \bar{z}_k)
\tag{5.7}
$$

Considering the kth piezoceramic layer and the coupled constitutive relations the piezoceramic force and moment vectors are given by

$$\left(\{N_\phi\}, \{M_\phi\}\right) = \int_{-h/2}^{h/2} \left[\overline{Q}\right]_k \{d\}_k E_{3k} (1, \overline{z}) d\overline{z}$$ (5.8)

6. Equations of Motion

Finite element equations of motion for the laminated composite panel with fully coupled electrical-structural properties are derived utilizing the generalized Hamilton's principle[4] to obtain

$$\int_1^2 \delta(T - U + W_e - W_m + W) dt = 0$$ (6.1)

where T and U are the kinetic energy and strain energy of the system, W_e is the electrical energy, W_m is the magnetic energy, and W is the work done due to external forces and applied electric field. The magnetic energy is negligible for piezoceramic materials if no external magnetic fields are located near the specimen. The kinetic energy of the shallow shell element is defined as

$$T = \int_V \frac{1}{2}\rho\left(\{\dot{w}\}^T\{\dot{w}\} + \{\dot{u}\}^T\{\dot{u}\} + \{\dot{v}\}^T\{\dot{v}\}\right)dV$$ (6.2)

where $\dot{w}$, $\dot{u}$, and $\dot{v}$ are the transverse and membrane velocity components and ρ is the mass per unit volume, and $-$ is the volume of the element. The potential and electrical energy are defined as

$$U = \int_V \frac{1}{2}\{\varepsilon\}^T\{\sigma\}dV$$ (6.3)

$$W_e = \int_V \frac{1}{2}\{E\}^T\{D\}dV$$ (6.4)

and the work done on the element by external sources is defined as

$$W = \int_V \{w\}^T\{F_b\}dV + \int_{S_1} \{w\}^T\{F_s\}dS + \{w\}^T\{F_c\} - \int_{S_2} V\rho_{cs}dS$$ (6.5)

8

where $\{F_b\}$ is the body force vector, $\{F_s\}$ is the surface traction vector. $\{F_c\}$ is the concentrated loading vector, S_1 is the surface area of the applied traction, S_2 is the surface area of the piezoelectric material, V is the voltage applied to the piezoceramic layer, and ρ_{cs} is the total electrical charge due to self-generated piezoelectricity and applied actuation voltage. In Hamilton's principle, all variations must vanish at the time $t = t_1$ and $t = t_2$. The Hamilton's variational statement may be written in the most general form as

$$\int_V \left(\rho \left(\{\delta \dot{w}\}^T \{\dot{w}\} + \{\delta \dot{u}\}^T \{\dot{u}\} + \{\delta \dot{v}\}^T \{\dot{v}\} \right) \right.$$

$$- \{\delta \varepsilon\}^T \{\sigma\} + \{\delta E\}^T \{D\} + \{\delta w\}^T \{F_b\} \right] dV$$

$$+ \int_{S_1} \{\delta w\}^T \{F_s\} dS - \int_{S_2} \delta V \rho_{cs} dS + \{\delta w\}^T \{F_c\} = 0 \tag{6.6}$$

Evaluation of Eq. (6.6) leads to the development of the finite element matrices and the elemental equations of motion. Employing the stress resultants, the variational potential and electrical energy may be described as

$$\delta (U - W_e) = \int_A \left(\{\delta \varepsilon^o\}^T \{N\} + \{\delta \kappa\}^T \{M\} + \alpha \{\delta \gamma\}^T \{R\} - \{\delta E\}^T \{D\} \right) dA \tag{6.7}$$

where the shear correction factor for the MIN6 element is defined as

$$\alpha = \frac{1}{1 + \frac{1}{2} \sum_{i=4,9} k_{s_{ii}} / \sum_{j=4,9} k_{b_{jj}}} \tag{6.8}$$

The finite element equations can be determined by completing the variational work statement in terms of the nodal values. Furthermore, it is convenient to specify the shallow shell slope matrix in the following form

$$[\theta_o] = \begin{bmatrix} h_o{,}_x & 0 \\ 0 & h_o{,}_y \\ h_o{,}_y & h_o{,}_x \end{bmatrix} \tag{6.9}$$

9

where $h_o = h_o(x,y)$ and is the constant shallow shell geometry. The stress resultants are written in nodal components, Eq. (5.5) as follows

$$\{N\} = [A]\{\varepsilon^o\} + [B]\{\kappa\} - \{N_\phi\}$$
$$= [A][C_m]\{w_m\} - [A][\theta_o]\{\theta\} + [B][C_b]\{\theta\} - \{N_\phi\} \tag{6.10}$$

$$\{M\} = [B]\{\varepsilon^o\} + [D]\{\kappa\} - \{M_\phi\}$$
$$= [B][C_m]\{w_m\} - [B][\theta_o]\{\theta\} + [D][C_b]\{\theta\} - \{M_\phi\} \tag{6.11}$$

$$\{R\} = [A_s][C_{\gamma b}]\{w_b\} + [A_s][C_{\gamma \theta}]\{\theta\} \tag{6.12}$$

Variation of the electrical energy requires attention due to z dependence

$$\int_A \left[\int_{-h/2}^{h/2} \left[(\delta E_{3k}) D_{3k} d\bar{z} \right] \right] dA =$$
$$\int_A \left[\sum_{k=1}^{np} \int_{\bar{z}_k}^{\bar{z}_{k+1}} \left[(\delta E_{3k}) \{d\}_k^T [\bar{Q}]_k \left(\{\varepsilon^0\} + \bar{z}\{\kappa\} - E_{3k}\{d\}_k \right) + \epsilon_{33k}^\sigma E_{3k} \right] d\bar{z} \right] dA \tag{6.13}$$

Completing the integration with respect to z yields

$$\int_A \left[\sum_{k=1}^{np} \left[(\delta E_{3k})\{d\}_k^T [\bar{Q}]_k h_k \{\varepsilon^o\} + (\delta E_{3k})\{d\}_k^T [\bar{Q}]_k \{\kappa\} \frac{h_k}{2}(\bar{z}_{k+1} + \bar{z}_k) \right. \right.$$
$$\left. \left. - (\delta E_{3k})\{d\}_k^T [\bar{Q}]_k \{d\}_k E_{3k} h_k + (\delta E_{3k}) \epsilon_{33k}^\sigma E_{3k} h_k \right] \right] dA \tag{6.14}$$

Before continuing, we can further expand the definitions of the piezoelectric force and moment vectors. The force vector may be expressed as

$$\{N_\phi\} = \sum_{k=1}^{np} [\bar{Q}]_k \{d\}_k h_k E_{3k}$$
$$= \left[[\bar{Q}]_1 \{d\}_1 h_1 \quad \cdots \quad [\bar{Q}]_k \{d\}_k h_k \quad \cdots \quad [\bar{Q}]_{np} \{d\}_{np} h_{np} \right] \{E_3\}$$
$$= -\left[[\bar{Q}]_1 \{d\}_1 h_1 \quad \cdots \quad [\bar{Q}]_k \{d\}_k h_k \quad \cdots \quad [\bar{Q}]_{np} \{d\}_{np} h_{np} \right] [B_\phi] \{w_\phi\}$$
$$= -[P_N][B_\phi]\{w_\phi\} \tag{6.15}$$

Similarly, the piezoelectric moment vector can be expressed as

$$\{M_\phi\} = -[P_M][B_\phi]\{w_\phi\} \tag{6.16}$$

where

$$[P_M] = \left[\frac{1}{2}[\overline{Q}]_1 \{d\}_1 h_1(\overline{z}_2 + \overline{z}_1) \quad \cdots \quad \frac{1}{2}[\overline{Q}]_k \{d\}_k h_k(\overline{z}_{k+1} + \overline{z}_k) \quad \cdots \right.$$
$$\left. \frac{1}{2}[\overline{Q}]_{np} \{d\}_{np} h_{np}(\overline{z}_{np+1} + \overline{z}_{np})\right] \tag{6.17}$$

Eq.(6.14) can be recast in matrix form using the above definitions as

$$= \int_A \{\delta E_3\}^T \left([P_N]^T \{\varepsilon^o\} + [P_M]^T \{\kappa\} - [\chi][B_\phi]^{-1}\{E_3\} + [\epsilon_{33}^\sigma][B_\phi]^{-1}\{E_3\}\right) dA \tag{6.18}$$

where

$$[\chi] = \begin{bmatrix} \{d\}_1^T[\overline{Q}]_1\{d\}_1 & \cdots & 0 \\ \vdots & \{d\}_k^T[\overline{Q}]_k\{d\}_k & \vdots \\ 0 & \cdots & \{d\}_{np}^T[\overline{Q}]_{np}\{d\}_{np} \end{bmatrix} \tag{6.19}$$

Thus, the expansion of the variational potential and electrical energy can be achieved by substituting the aforementioned relations as follows

$$\delta(U - W_e) = \int_A \left(\{\delta\varepsilon^o\}^T \{N\} + \{\delta\kappa\}^T \{M\} + \alpha\{\delta\gamma\}^T \{R\} - \{\delta E\}^T \{D\}\right) dA$$

$$= \int_A \left\{\left(\{\delta w_m\}^T [C_m]^T - \{\delta\theta\}^T [\theta_o]^T\right)\left([A][C_m]\{w_m\} - [A][\theta_o]\{\theta\} + [B][C_b]\{\theta\} - \{N_\phi\}\right)\right.$$

$$+ \{\delta\theta\}^T [C_b]^T \left([B][C_m]\{w_m\} - [B][\theta_o]\{\theta\} + [D][C_b]\{\theta\} - \{M_\phi\}\right)$$

$$+ \alpha\left(\{\delta w_b\}^T [C_{\gamma b}]^T + \{\delta\theta\}^T [C_{\gamma\theta}]^T\right)\left([A_s][C_{\gamma b}]\{w_b\} + [A_s][C_{\gamma\theta}]\{\theta\}\right)$$

$$+ \{\delta w_\phi\}^T [B_\phi]^T \left[[P_N]^T [C_m]\{w_m\} + [P_N]^T [\theta_o]\{\theta\} + [P_M]^T [C_b]\{\theta\}\right.$$

$$\left.\left. + \left([\epsilon_{33}^\sigma] - [\chi]\right)\{w_\phi\}\right]\right\} dA \tag{6.20}$$

Expanding Eq.(6.20) term by term yields expressions leading to the element stiffness matrices

$$= \int_A \left\{ \{\delta w_m\}^T [C_m]^T [A][C_m]\{w_m\} \right. \tag{6.21}$$

$$- \{\delta w_m\}^T [C_m]^T [A][\theta_o]\{\theta\} \tag{6.22}$$

$$+ \{\delta w_m\}[C_m]^T [B][C_b]\{\theta\} \tag{6.23}$$

$$+ \{\delta w_m\}[C_m]^T [P_N][B_b]\{w_\phi\} \tag{6.24}$$

$$- \{\delta \theta\}^T [\theta_o]^T [A][C_m]\{w_m\} \tag{6.25}$$

$$+ \{\delta \theta\}^T [\theta_o]^T [A][\theta_o]\{\theta\} \tag{6.26}$$

$$- \{\delta \theta\}^T [\theta_o]^T [B][C_b]\{\theta\} \tag{6.27}$$

$$+ \{\delta \theta\}^T [\theta_o]^T [P_N][B_\phi]\{w_\phi\} \tag{6.28}$$

$$+ \{\delta \theta\}^T [C_b]^T [B][C_m]\{w_m\} \tag{6.29}$$

$$- \{\delta \theta\}^T [C_b]^T [B][\theta_o]\{\theta\} \tag{6.30}$$

$$+ \{\delta \theta\}^T [C_b]^T [D][C_b]\{\theta\} \tag{6.31}$$

$$+ \{\delta \theta\}^T [C_b][P_M][B_\phi]\{w_\phi\} \tag{6.32}$$

$$+ \alpha \{\delta w_b\}^T [C_{yb}]^T [A_s][C_{yb}]\{w_b\} \tag{6.33}$$

$$+ \alpha \{\delta w_b\}^T [C_{yb}]^T [A_s][C_{y\theta}]\{\theta\} \tag{6.34}$$

$$+ \alpha \{\delta \theta\}^T [C_{y\theta}]^T [A_s][C_{yb}]\{w_b\} \tag{6.35}$$

$$+ \alpha \{\delta \theta\}^T [C_{y\theta}]^T [A_s][C_{y\theta}]\{\theta\} \tag{6.36}$$

$$- \{\delta w_\phi\}^T [B_\phi]^T [P_N]^T [C_m]\{w_m\} \tag{6.37}$$

$$- \{\delta w_\phi\}^T [B_\phi]^T [P_N]^T [\theta_o]\{\theta\} \tag{6.38}$$

$$- \{\delta w_\phi\}^T [B_\phi]^T [P_M]^T [C_b]\{\theta\} \tag{6.39}$$

$$\left. + \{\delta w_\phi\}^T [B_\phi]^T ([\epsilon_{33}^\sigma] - [\chi])\{w_\phi\} \right\} dA \tag{6.40}$$

Completing the generalized Hamilton's principle considering nodal degrees-of-freedom yields inertia, external mechanical loading and piezoceramic actuation quantities

12

$$\delta W_{external} = \int_A \left\{ \left(\{\delta w_b\}^T \{H_w\} + \{\delta \theta\}^T \{H_{w\theta}\} \right) \left(p(x,y,t) - \rho \left(\lfloor H_w \rfloor \{\ddot{w}_b\} + \lfloor H_{w\theta} \rfloor \{\ddot{\theta}\} \right) \right) \right.$$
$$\left. - \rho \{\delta w_m\}^T \left(\{H_u\} \lfloor H_u \rfloor \{\ddot{w}_m\} - \{H_v\} \lfloor H_v \rfloor \{\ddot{w}_m\} \right) \right\} dA - \int_{S_p} \{\delta w_\phi\}^T \{\rho_{cs}\} dA \qquad (6.41)$$

Finite element stiffness matrices result from examination of the potential and electrical energies of the variational work statement. Each stiffness matrix, including fully coupled electrical-structural and geometrical shallow shell stiffness' is defined from the indicated term of Eqs.(6.21)-(6.41)

$$\{\delta\theta\}^T [k_\theta]\{\theta\} \text{ where } [k_\theta] = \int_A [C_b]^T [D][C_b] dA \qquad (6.42)$$

$$\{\delta\theta\}^T [k_{\theta m}]\{w_m\} \text{ where } [k_{\theta m}] = \int_A [C_b]^T [B][C_m] dA \qquad (6.43)$$

$$\{\delta w_m\}[k_{m\theta}]\{\theta\} \text{ where } [k_{m\theta}] = \int_A [C_m]^T [B][C_b] dA \qquad (6.44)$$

$$\{\delta w_m\}^T [k_m]\{w_m\} \text{ where } [k_m] = \int_A [C_m]^T [A][C_m] dA \qquad (6.45)$$

$$\{\delta w_m\}[k_{m\phi}]\{w_\phi\} \text{ where } [k_{m\phi}] = \int_A [C_m] \llbracket P_N \rrbracket [B_\phi] dA \qquad (6.46)$$

$$\{\delta w_\phi\}^T [k_{\phi m}]^T \{w_m\} \text{ where } [k_{\phi m}] = \int [B_\phi]^T [P_N]^T [C_m] dA \qquad (6.47)$$

geometric stiffness due to shallow shell geometry

$$\{\delta w_m\}^T [k_{m\theta}]_o \{\theta\} \text{ where } [k_{m\theta}]_o = \int_A [C_m]^T [A][\theta_o] dA \qquad (6.48)$$

$$\{\delta\theta\}^T [k_{\theta m}]_o \{w_m\} \text{ where } [k_{\theta m}]_o = \int_A [\theta_o]^T [A][C_m] dA \qquad (6.49)$$

$$\{\delta\theta\}^T [k_\theta]_o \{\theta\} \text{ where } [k_\theta]_o = \int_A \left([\theta_o]^T [A][\theta_o] - [\theta_o]^T [B][C_b] - [C_b]^T [B][\theta_o] \right) dA \qquad (6.50)$$

$$\{\delta\theta\}^{T}\left[k_{\theta\phi}\right]_{o}\{w_{\phi}\} \quad \text{where} \quad \left[k_{\theta\phi}\right]_{o} = \int_{A}\left[\theta_{o}\right]^{T}\left[P_{N}\right]\left[B_{\phi}\right]dA \tag{6.51}$$

$$\{\delta w_{\phi}\}^{T}\left[k_{\phi\theta}\right]_{o}\left[\theta_{o}\right]\{\theta\} \quad \text{where} \quad \left[k_{\phi\theta}\right]_{o} = \int_{A}\left[B_{\phi}\right]^{T}\left[P_{N}\right]^{T}\left[\theta_{o}\right]dA \tag{6.52}$$

stiffness due to shear effects

$$\alpha\{\delta\theta\}^{T}\left[k_{s_{o}}\right]\{\theta\} \quad \text{where} \quad \left[k_{s_{o}}\right] = \int_{A}\left[C_{\gamma\theta}\right]^{T}\left[A_{s}\right]\left[C_{\gamma\theta}\right]dA \tag{6.53}$$

$$\alpha\{\delta\theta\}^{T}\left[k_{s_{ob}}\right]\{w_{b}\} \quad \text{where} \quad \left[k_{s_{ob}}\right] = \int_{A}\left[C_{\gamma\theta}\right]^{T}\left[A_{s}\right]\left[C_{\gamma b}\right]dA \tag{6.54}$$

$$\alpha\{\delta w_{b}\}^{T}\left[k_{s_{bo}}\right]\{\theta\} \quad \text{where} \quad \left[k_{s_{bo}}\right] = \int_{A}\left[C_{\gamma b}\right]^{T}\left[A_{s}\right]\left[C_{\gamma\theta}\right]dA \tag{6.55}$$

$$\alpha\{\delta w_{b}\}^{T}\left[k_{s_{b}}\right]\{w_{b}\} \quad \text{where} \quad \left[k_{s_{b}}\right] = \int_{A}\left[C_{\gamma b}\right]^{T}\left[A_{s}\right]\left[C_{\gamma b}\right]dA \tag{6.56}$$

coupled piezoelectric-structural stiffness

$$\{\delta\theta\}^{T}\left[k_{\theta\phi}\right]\{w_{\phi}\} \quad \text{where} \quad \left[k_{\theta\phi}\right] = \int_{A}\left[C_{b}\right]^{T}\left[P_{M}\right]\left[B_{\phi}\right]dA \tag{6.57}$$

$$\{\delta w_{\phi}\}^{T}\left[k_{\phi\theta}\right]\{\theta\} \quad \text{where} \quad \left[k_{\phi\theta}\right] = \int_{A}\left[B_{\phi}\right]^{T}\left[P_{M}\right]^{T}\left[C_{b}\right]dA \tag{6.58}$$

$$\{\delta w_{\phi}\}^{T}\left[k_{\phi}\right]\{w_{\phi}\} \quad \text{where} \quad \left[k_{\phi}\right] = \int_{A}\left[B_{\phi}\right]^{T}\left(\left[\epsilon_{33}^{\sigma}\right]-\left[\chi\right]\right)dA \tag{6.59}$$

mass matrices and load vectors from Eq. (6.41)

$$\left[m_{b}\right] = \int_{A}\left[H_{w}\right]^{T}\rho\left[H_{w}\right]dA \tag{6.60}$$

$$\left[m_{b\theta}\right] = \int_{A}\left[H_{w}\right]^{T}\rho\left[H_{w\theta}\right]dA \tag{6.61}$$

$$\left[m_{\theta b}\right] = \int_{A}\left[H_{w\theta}\right]^{T}\rho\left[H_{w}\right]dA \tag{6.62}$$

$$\left[m_{\theta}\right] = \int_{A}\left[H_{w\theta}\right]^{T}\rho\left[H_{w\theta}\right]dA \tag{6.63}$$

$$[m_m] = \int_A ([H_u] + [H_u])^T \rho ([H_u] + [H_u]) dA \qquad (6.64)$$

$$\{p_b(t)\} = \int_A [H_w]^T p(x,y,t) dA \qquad (6.65)$$

$$\{p_\theta(t)\} = \int_A [H_{w\theta}]^T p(x,y,t) dA \qquad (6.66)$$

$$\{p_\phi(t)\} = -\int_A \rho_{cs} dA \qquad (6.67)$$

Resulting in the following finite element equation of motion

$$\begin{bmatrix} [m_b] & [m_{b\theta}] & 0 & 0 \\ [m_{\theta b}] & [m_\theta] & 0 & 0 \\ 0 & 0 & 0 & [m_m] \\ 0 & 0 & 0 & 0 \end{bmatrix} \begin{Bmatrix} \ddot{w}_b \\ \ddot{\theta} \\ \ddot{w}_m \\ \ddot{w}_\phi \end{Bmatrix} + \left(\begin{bmatrix} 0 & 0 & 0 & 0 \\ 0 & [k_\theta]+[k_\theta]_o & [k_{\theta m}]+[k_{\theta m}]_o & [k_{\theta\phi}]+[k_{\theta\phi}]_o \\ 0 & [k_{m\theta}]-[k_{m\theta}]_o & [k_m] & [k_{m\phi}] \\ 0 & [k_{\phi b}]-[k_{\phi b}]_o & [k_{\phi m}] & [k_\phi] \end{bmatrix} \right.$$

$$\left. + \alpha \begin{bmatrix} [k_{s_b}] & [k_{s_{b\theta}}] & 0 & 0 \\ [k_{s_{\theta b}}] & [k_{s_\theta}] & 0 & 0 \\ 0 & 0 & 0 & 0 \\ 0 & 0 & 0 & 0 \end{bmatrix} \right) \begin{Bmatrix} w_b \\ \theta \\ w_m \\ w_\phi \end{Bmatrix} = \begin{Bmatrix} p_b(t) \\ p_\theta(t) \\ 0 \\ p_\phi(t) \end{Bmatrix} \qquad (6.68)$$

Through standard finite element assembly lead to

$$\begin{bmatrix} M & 0 \\ 0 & 0 \end{bmatrix} \begin{Bmatrix} \ddot{W} \\ \ddot{W}_\phi \end{Bmatrix} + \begin{bmatrix} K_w & K_{w\phi} \\ K_{\phi w} & K_\phi \end{bmatrix} \begin{Bmatrix} W \\ W_\phi \end{Bmatrix} = \begin{Bmatrix} P_w \\ P_\phi \end{Bmatrix} \qquad (6.69)$$

Separation of Eq.(6.69) produces two coupled equations of motions

$$[M]\{\ddot{W}\} + ([K_w] - [K_{w\phi}][K_\phi]^{-1}[K_{\phi w}])\{W\} = \{P_w\} - [K_{w\phi}][K_\phi]^{-1}\{P_\phi\} \qquad (6.70)$$

$$\{W_\phi\} = [K_\phi]^{-1}\{P_\phi\} - [K_\phi]^{-1}[K_{\phi w}]\{W\} \qquad (6.71)$$

15

Eq.(6.70) describes the system with respect to the primary variable $\{W\}$, the structural nodal dof, and the applied loads, indicated by the $\{P_w\}, [K_{w\phi}][K_\phi]^{-1}\{P_\phi\}$. Subsequently, Eq.(6.71) defines the electrical dof as a function both the structural dof and the external actuation voltage. Thus, finite element formulation supports simultaneous sensing and actuation. However, if the piezoceramic patches are restricted to actuation or sensing only, the fully coupled formulation is preserved.

7. Modal Formulation

The number of nodal degrees of freedom can be excessively large and thus impede the controller design and computational efficiency. However, the modal coordinate transformation can be utilized by considering the overall structural response can be very well represented by a reduced number of normal modes. Thus, expressing Eqs. (6.70) and (6.71) in the modal domain yields

$$[M_r]\{\ddot{q}\} + [C_r]\{\dot{q}\} + [K_r] = \{F_{rw}\} - \{F_{r\phi}\} \tag{7.1}$$

$$\{W_\phi\} = [K_\phi]^{-1}\{P_\phi\} - [K_\phi]^{-1}[K_{\phi w}][\psi]\{q\} \tag{7.2}$$

where; $[M_r] = [\psi]^T[M][\psi]$, $[K_r] = [\psi]^T([K_w] - [K_{w\phi}][K_\phi]^{-1}[K_{\phi w}])[\psi]$, $\{F_{rw}\} = [\psi]^T\{P_w\}$,

and $\{F_{r\phi}\} = [\psi]^T[K_{w\phi}][K_\phi]^{-1}\{P_\phi\}$. The damping matrix $[C_r]$ will be determined experimentally from the corresponding damping ratios of the individual modes measured. The modal matrix, or eigenvectors, $[\psi]$ represents a reduced set of the first ten normal modes. Hence, the large number of finite element equations simply reduces to ten equations in the modal domain.

8. Development of Actuator Location Optimization Process

The piezoelectric modal actuator participation (PMAP) $[M]^{-1}[\psi]^T[K_{u\phi}][K_\phi]^{-1}\{P_\phi(t)\}$

indicates the contribution of the actuators to each of the modes. Exploiting the coupled

electrical-structural formulation and the modal domain properties the PMAP is evaluated

and ranked for desired acoustical modal contribution. Hence, the preferred actuator

location is determined. Results determined using a rectangular 24-dof plate finite

element with three piezoceramic patches are shown in Table 1. The patch numbering

refers to Figure 2, where patch 2 is indicated by a 2, and patches 8 and 9 are shown by 8

and 9 respectively. Note that patch 9 consist of nine finite elements and patches 2 and 8

each have one element. Furthermore, each acoustic radiating mode is indicated along

with the corresponding PMAP. The PMAP values indicated in Table 1 are normalized

indicating the maximum actuator performance for mode (1,3) with patch 9. The

piezoceramic stress values $d_{31}=d_{32}=0.171e-9$ was used and is representative of PZT-5A[5].

Patch 2	Patch 8	Patch 9	Mode	
0.2151	0.2151	-0.8134	(1,1)	
0.0901	0.0901	-1.0000	(1,3)	
0.0562	0.0562	0.2868	(3,1)	
-0.0592	-0.0592	0.0072	(5,1)	
-0.0747	-0.0747	-0.2661	(3,3)	
-0.1326	0.1326	-0.0000	(4,3)	

Table 1 PAMP for 10"x14"x0.040" rectangular plate

nap2 =

$$
\begin{bmatrix}
1 & 1 & 1 & 1 & 1 & 1 & 1 & 2 & 1 \\
1 & 1 & 1 & 1 & 1 & 1 & 1 & 1 & 1 \\
1 & 1 & 1 & 9 & 9 & 9 & 1 & 1 & 1 \\
1 & 1 & 1 & 9 & 9 & 9 & 1 & 1 & 1 \\
1 & 1 & 1 & 9 & 9 & 9 & 1 & 1 & 1 \\
1 & 1 & 1 & 1 & 1 & 1 & 1 & 1 & 1 \\
1 & 8 & 1 & 1 & 1 & 1 & 1 & 1 & 1
\end{bmatrix}
$$

Figure 2 Vector representing typical piezoceramic sensor-actuator location map of three

patches. Key: (1) no piezoceramic present, (2) a single patch, (8) a single patch, and (9)

patch comprised of nine finite elements.

9. COUPLED ACOUSTICS USING RADIATION FILTERS

The structural velocity distribution may be constructed by superposition of a set of

independent acoustic modal velocities[6]. The acoustic velocity modes correspond to the

acoustic pressure distributions of the radiated sound of the structure. Thus, a radiation

filter may be constructed by considering a radiation operator which represents

independent discrete acoustic structural radiators. The radiation operator is frequency

dependent and may be subjected to a singular value decomposition, which yields

interesting and useful results. Consider the following relationship of the total radiated

power of a vibrating structure

$$\{P\} = \{v(j\omega)\}^H [R(j\omega)]\{v(j\omega)\} \tag{9.1}$$

where $\{v(j\omega)\}$ is a $nx1$ vector of nodal velocities and $[R(j\omega)]$ is a nxn radiation matrix.

The radiation matrix is proportional to the radiation resistance with diagonal and off

diagonal elements corresponding to self and mutual radiation resistance respectively.

Thus, a vibrating structure represented by n discrete independent acoustic point sources

or radiators represented by the following radiation matrix

18

$$[R] = \frac{\omega^2 \rho_o A^2}{4\pi c} \begin{bmatrix} 1 & \dfrac{\sin(kr_{12})}{kr_{12}} & \cdots & \dfrac{\sin(kr_{1n})}{kr_{1n}} \\ \dfrac{\sin(kr_{21})}{kr_{21}} & 1 & \dfrac{\sin(kr_{23})}{kr_{23}} & \vdots \\ \vdots & \vdots & \ddots & \vdots \\ \dfrac{\sin(kr_{n1})}{kr_{n1}} & \cdots & \dfrac{\sin(kr_{nn-1})}{kr_{nn-1}} & 1 \end{bmatrix} \tag{9.2}$$

where ω is the circular frequency, ρ_o is the density of air, A is the elemental area of the corresponding radiator, c the speed of sound in air, k the wave number (ω/c), and r_{pq} is the distance between the pth and q^{th} velocity location. Singular value decomposition of the radiation matrix yields dominant acoustic radiation modes for each frequency. Thus

$$[R(j\omega)] = [u][\Sigma][u]^H \tag{9.3}$$

where $[u] = [\{u\}_1 \quad \{u\}_2 \quad \cdots \quad \{u\}_n]$ is a $n \times n$ matrix whose column represent normalized acoustic radiation modes at ω_p and $[\Sigma]$ is a $n \times n$ matrix of singular values. The magnitude of the qth singular value indicates the relative importance of the corresponding acoustic radiation mode. The singular values, as a function of frequency, represent the dominant coupled acoustic modes, which provides guidance for developing a noise control strategy. The associated normalized singular vectors obtained from the singular value decomposition represent the contributing acoustic radiation mode. Figure 4 shows the dominate acoustic radiation modes determined by evaluating the radiation matrix singular values. Furthermore, Figure 5 presents the dominant corresponding acoustical SVD radiation modes.
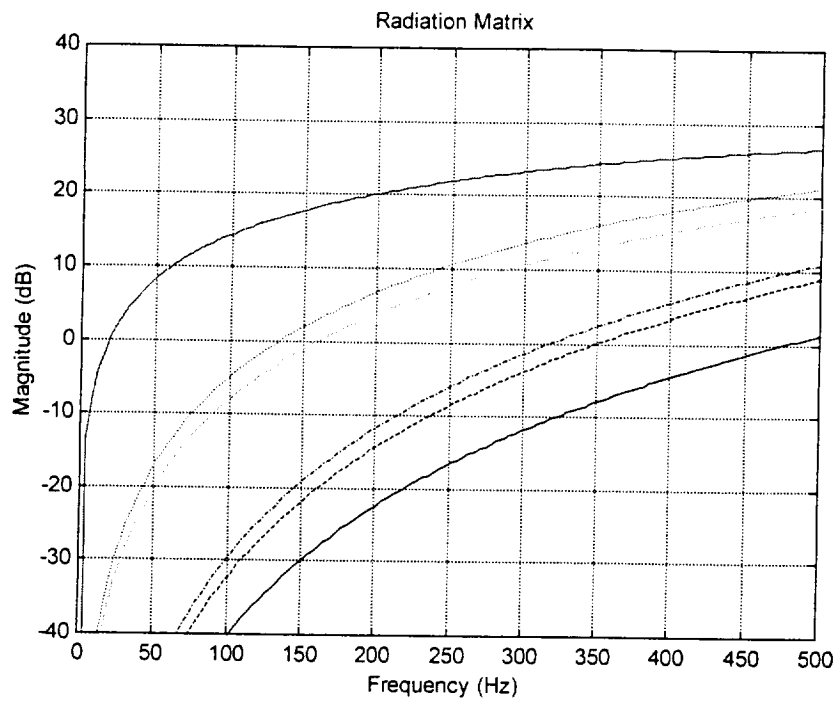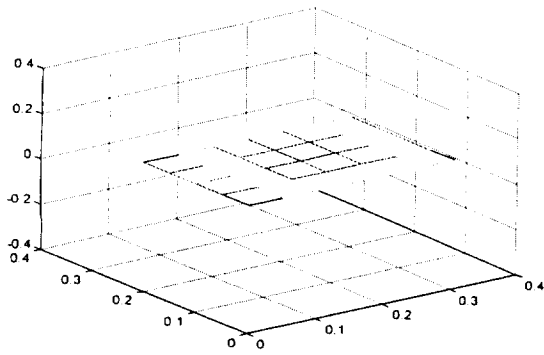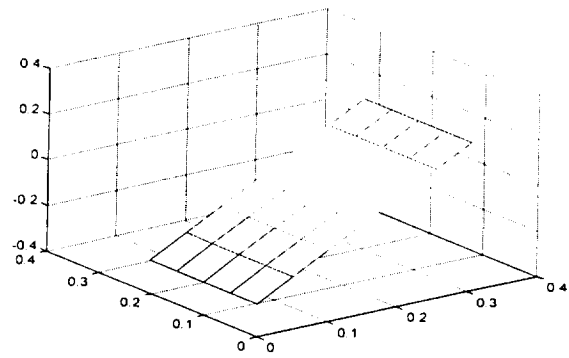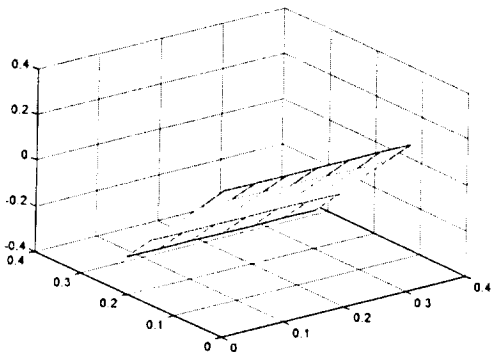
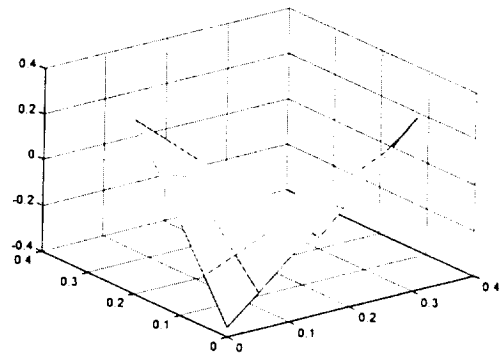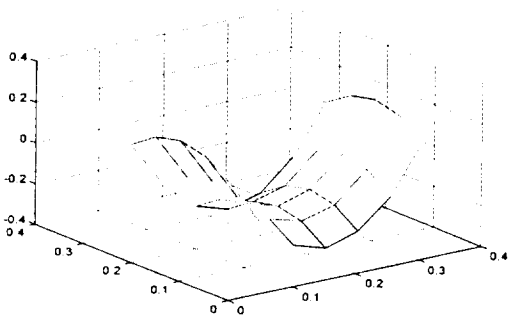Figure 5 Dominant Acoustic Radiation Modes

Mode 1

Mode 2

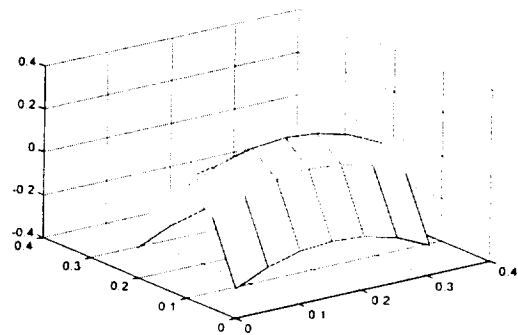Mode 3

Mode 4

Mode 5

Mode 6

Figure 6 Acoustic Radiation SVD Mode Shapes

10. Control Strategy

The objective of this research emphasizes determining the preferred placement of piezoceramic sensors and actuators locations to minimizing the structure-borne radiated noise of a cylindrical shell, to this end $\mathcal{H}_2$ and LQG[7] control strategies will be employed. The $\mathcal{H}_2$ and LQG has been well researched and applied to laboratory experiments. Although it may not represent the best practical control approach much data has been published and will provide guidance. The state space approach is achievable by considering the following fully coupled equations of motion

$$[M]\{\ddot{W}\} + ([K_W] - [K_{w\phi}][K_\phi]^{-1}[K_{\phi w}] - [K_{N\phi}])\{W\} = \{P_w(t)\} - [K_{w\phi}][K_\phi]^{-1}\{P_\phi(t)\} \tag{10.1}$$

Using a modal transformation results in the following set of uncoupled modal equations

$$\ddot{q}_r + 2\zeta_r\omega_r\dot{q}_r + \omega_r^2 q_r = \frac{f_r}{m_r} \tag{10.2}$$

Where the modal mass and stiffness are obtained from

$$\{\psi\}_r^T([M], [K])\{\psi\}_r = (m_r, k_r) \text{ where } [K] = ([K_w] - [K_{w\phi}][K_\phi]^{-1}[K_{\phi w}] - [K_{N\phi}]) \tag{10.3}$$

and

$$f_r = \{\psi\}_r^T(\{P_w(t)\} - [K_{w\phi}][K_\phi]^{-1}\{P_\phi(t)\}) \tag{10.4}$$

The following state space equations for LQG can be utilized

$$\{\dot{x}(t)\} = [A]\{x(t)\} + [B_u]\{u(t)\} + [B_w]\{w(t)\} \tag{10.5}$$

22

$$\{y(t)\} = [C]\{x(t)\} + \{v(t)\}, \qquad \{x\} = \{q \quad \dot{q}\}^{T}$$

where the following state space transformation was applied to the finite element coupled equations of motion

$$[A] = \begin{bmatrix} [0] & [I] \\ -[M_r]^{-1}[K_r] & -[M_r]^{-1}[C_r] \end{bmatrix}$$

$$[B_u] = \begin{bmatrix} [0] \\ [[M_r]^{-1}[\psi]^T[K_{w\phi}][K_\phi]^{-1}] \end{bmatrix} \quad [B_w] = \begin{bmatrix} [0] \\ [M_r]^{-1}[\psi]^T \end{bmatrix} \tag{10.6}$$

$$[C] = [[K_\phi]^{-1}[K_{\phi w}][\psi] \quad [0]]$$

Evaluation of the system corresponding to the previous piezoceramic patches was conducted by observing the open loop impulse response as shown in Figure 7. Each patch is shown in Figure 2 and designated by 2,8, and 9. Again, the data represents a structure modeled using rectangular plate elements modified to include the couple electrical-structural formulation.